Original Article

Glucagon-Like Peptide 1 Regulates Sequential and Compound Exocytosis in Pancreatic Islet β-Cells

Edwin P. Kwan and Herbert Y. Gaisano

Glucagon-like peptide 1 (GLP-1) has been postulated to potentiate insulin secretion by cAMP-mediated enhancement of mobilization and priming of secretory granules, but the precise exocytic events are unknown. We used epi-fluorescent microscopy of the fluorescent dye FM1-43, which incorporates into the plasma membrane and the exocytosing secretory granules (appearing as plasma membrane hotspots). KCl evoked exocytosis of 1.8 ± 0.5 hotspots/rat β-cell at the cell periphery, 82% of which are single transient increases of low amplitudes (151 ± 7%), suggesting single secretory granule exocytosis; and the remaining 18% are stepwise increases in plasma membrane hotspots with higher amplitudes (170 ± 9%), suggesting sequential secretory granule to secretory granule exocytic fusions. Addition of GLP-1 increased the hotspots to 6.0 ± 0.7/β-cell and exhibited a larger number of stepwise (41%) than transient (10%) increases with higher amplitudes of 259 ± 19 and 278 ± 23%, respectively. More interestingly, GLP-1 also evoked a robust and sustained pattern (49%) with even higher amplitudes of 354 ± 18%, which are likely accelerated sequential secretory granule–secretory granule fusions. Electron microscopy studies collaborated with these imaging results, showing that GLP-1 increased the number of docked secretory granules at the plasma membrane and also increased the number of events showing direct contact of oncoming secretory granules with secretory granules undergoing exocytosis. We conclude that the potentiation of insulin secretion by GLP-1 is contributed by the mobilization of more insulin secretory granules to dock at the plasma membrane and the acceleration of sequential secretory granule–secretory granule fusions. ***Diabetes*** **54:2734–2743, 2005**

From the Departments of Medicine and Physiology, University of Toronto, Toronto, Ontario, Canada

Address correspondence and reprint requests to Dr. Herbert Y. Gaisano, University of Toronto, 1 Kings College Circle, Room 7226, Toronto, ON, Canada, M5S 1A8. E-mail: herbert.gaisano@utoronto.ca.

Received for publication 9 December 2004 and accepted in revised form 3 June 2005.

Additional information for this article can be found in an online appendix at http://diabetes.diabetesjournals.org.

DGG, docked granule-granule; EGG, exocytosing granule-granule; GLP-1, glucagon-like peptide 1; IBMX, isobutylmethylxanthine.

Food (glucose) ingestion results in the release of glucagon-like peptide 1 (GLP-1) from intestinal L-cells, which acts on the pancreatic islet β-cell to potentiate insulin secretion (1,2). On the β-cell, GLP-1 generates cAMP production, which augments insulin secretion, in part by enhancing the ATP-sensitive K^+ channel closure, L-type Ca^{2+} channel opening, and mobilization of intracellular Ca^{2+} stores [rev. in 2]. At the level of exocytosis, patch-clamp capacitance measurements have shown that cAMP activation, including that by GLP-1 stimulation, could amplify depolarization-evoked responses from single β-cells (3). Capacitance measurement measures the net change in cell surface area, which would underestimate the magnitude of exocytosis when endocytosis, which retrieves the plasma membrane, occurs concurrently (4) and would therefore be unable to examine insulin exocytosis after the first few minutes of stimulation.

The FM1-43 fluorescence imaging assay has been used to examine exocytosis at the levels of single vesicles/secretory granules fusion in nerve terminals (5,6), adrenal chromaffin cells (4), and lactotrophs (7). FM1-43 is a membrane-impermeable styryl dye that fluoresces when incorporated into the plasma membrane but not in solution. Hence, each exocytic event is visualized as a fluorescent "hotspot" when the dye stains the vesicular membrane upon fusion of a single secretory granule with the plasma membrane. We had previously tracked with high spatial and temporal resolution the FM1-43 exocytic events in single rat islet β-cells in response to K^+ depolarization and glucose (8). Confocal microscopy showed precise colocalization of the exocytosed insulin with the plasma membrane FM1-43 hotspots (8). In that study, K^+ depolarization evoked mostly single transient increases in plasma membrane FM1-43 fluorescence, whereas glucose evoked multi-stepwise increases, which we postulated to represent single insulin secretory granule exocytosis and sequential secretory granule–secretory granule exocytosis, respectively.

Here, we examined the exocytic events evoked by GLP-1 as determined by the FM1-43 imaging technique and then verified the precise exocytic events ultrastructurally by electron microscopy. Here, GLP-1 enabled K^+ depolarization to induce more plasma membrane hotspots and robust high-amplitude hotspots, which could be accounted for by electron microscopy to correspond to an increased

mobilization of insulin secretory granules toward and to dock onto the plasma membrane and to an increase in sequential secretory granule–secretory granule fusions, respectively. These results lead us to postulate that sequential secretory granule–secretory granule fusions are an effective mechanism of emptying more secretory contents (insulin) in a neuroendocrine cell type with few docked granules (i.e., islet β-cell) and that the docked granules undergoing exocytosis could serve to activate new docking sites for subsequent oncoming granules to fuse with.

RESEARCH DESIGN AND METHODS

Isolation of islets and cultures of β-cells. Islets from male Sprague-Dawley rats were isolated by collagenase digestion method as reported previously (9). The islets were dissociated into single cells using a Ca^{2+}/Mg^{2+}-free PBS (in 5 mmol/l EDTA) with 0.25 mg/ml trypsin for 10 min at 37°C with gentle shaking and then resuspended in enriched RPMI 1640 containing 2.8 mmol/l D-glucose at a density of 600,000 cells/ml. The resulting cell suspensions were plated on glass coverslips and allowed to adhere ~48 h before the imaging experiments were conducted.

FM1-43 epi-fluorescent imaging. Pancreatic β-cells cultured for 2–4 days were perfused with 4 μmol/l FM1-43 in nonstimulatory physiological bath solutions for ~5 min to achieve a basal and stable FM1-43 fluorescence staining evenly along the plasma membrane. The bath solutions consisted of 140 mmol/l NaCl, 2 mmol/l $CaCl_2$, 4 mmol/l KCl, 1 mmol/l $MgCl_2$, 10 mmol/l HEPES, and 2.5 mmol/l D-glucose, pH adjusted to 7.4 by NaOH. This basal FM1-43 fluorescence staining did not decrease over the usual duration of experiments that was tested in the absence of stimulus, indicating insignificant photobleaching of FM1-43. This concentration of FM1-43 was maintained in the extracellular media until near the end of the experiment when the cells were washed with FM1-43–free media to show that the FM1-43 incorporated into the plasma membrane could be reversibly washed out, indicating that the FM1-43 hotspots examined are due to exocytosis, and to confirm that no prominent endocytosis had occurred in the hotspots being examined. For stimulation, cells were triggered to depolarize by iso-osmotic 90-mmol/l KCl solutions (Na^+ substituted by K^+) with or without 10 nmol/l GLP-1 (7-36)-amide (Bachem, Torrance, CA) and/or 150 μmol/l isobutylmethylxanthine (IBMX) as specifically indicated. Fluorescent imaging experiments were performed with a system consisting of a Nikon TE2000U inverted microscope, a Hamamatsu ORCA-ER camera (6.45- × 6.45-μm physical pixels, giving 107.5 nm per image pixel with a 40× objective [1.3 NA] plus 1.5× lens inside the microscope body), and a Pentium IV computer with Simple PCI image acquisition and analysis software (Compix Imaging Systems, Cranberry Township, PA). Fluorescent images were obtained with 470/20-nm excitation and 515-nm long-pass emission filters. Exposure lasted ~0.2 s, and images were acquired at ~0.33 Hz. The experimental recordings were analyzed by obtaining the average fluorescence intensity values within the region of interests chosen to center around the hotspots and include only the plasma membrane throughout the course of the experiment. Background changes in fluorescence were monitored and subtracted from changes in cell membrane fluorescence.

Electron microscopy. Dispersed single cells obtained from ~200 islets per rat were cultured on culture dishes and were stimulated for 3 min with 90 mmol/l KCl + 150 μmol/l IBMX in the absence or presence of 10 nmol/l GLP-1 (7-36)-amide. They were then fixed with a Karnovsky style fixative (4% paraformaldehyde + 2.5% glutaraldehyde in a 0.1 mol/l cacodylate buffer with 5 mmol/l $CaCl_2$, pH 6.8) for 1 h, postfixed with 1% osmium tetroxide for 30 min, and treated with 2.5% uranyl acetate for 30 min. The cells were then dehydrated and infiltrated with Epon 812 resin. Completion of polymerization of the epoxy resin resulted in a solid epoxy disk, which was subjected to ultrathin sectioning (~80 nm) using a Reichert Ultracut E microtome, and collected on 300 mesh copper grids. The sections were counterstained using saturated uranyl acetate followed by Reynold's lead citrate and then examined and photographed in an Hitachi H7000 transmission electron microscope at an accelerating voltage of 75 kV. The granule diameter was estimated using the method previously described (10,11).

Statistics. Data are expressed as means ± SE. Statistical comparisons were performed by *t* test or ANOVA in which an acceptable level of significance was considered at $P < 0.05$.

TABLE 1
Number of exocytotic FM1–43 hotspots on the plasma membrane at the equatorial plane of rat pancreatic islet β-cells evoked by different agonists

Agonists	Hotspots per equatorial plane per cell
90 mmol/l KCl	1.8 ± 0.5
90 mmol/l KCl + 150 μmol/l IBMX	2.0 ± 0.3
10 nmol/l GLP-1 + 90 mmol/l KCl + 150 μmol/l IBMX	6.0 ± 0.7

Data are means ± SE.

RESULTS

KCl stimulation of rat islet β-cells evokes monophasic and sequential exocytosis. We first examined the effects of 90 mmol/l KCl alone on depolarization-evoked exocytosis in rat islet β-cells. KCl alone elicited an average of 1.8 ± 0.5 FM1-43 hotspots/cell ($n = 28$ hotspots from 13 of 16 consecutive cells analyzed) at the cell equator (Table 1). Of the 16 consecutive cells analyzed, 3 cells did not show any hotspot. As previously described (8), these plasma membrane FM1-43 hotspots were categorized as monophasic or multiphasic events based on the patterns of their rise to a peak and subsequent decline and based on the life spans of the fluorescent hotspots. The monophasic events were shorter lived (lasting for <200 s) before the plasma membrane FM1-43 fluorescent hotspots returned to basal membrane fluorescence levels, whereas FM1-43 membrane fluorescence in the multiphasic events increased in a stepwise fashion and reached a higher peak amplitude than the monophasic events. We had suggested that the monophasic events exhibiting a lower peak amplitude represent single insulin granule exocytic fusions (8), whereby the FM1-43 dye permeates into the exocytosing secretory granule membrane and likely also the core matrix, as was described in a similar lactotroph study (7). This is followed by a rapid dissolution of the FM1-43 dye into the cell exterior, which would correspond to the dissipation of the insulin core contents to the cell exterior. The multiphasic responses were considered as sequential fusions of insulin granules to previously exocytosed insulin granules. In sequential exocytosis, a variable amount of time is required for subsequent granules to be mobilized and/or primed for fusion and hence a delay in the increase in FM1-43 fluorescence as indicated by the plateaus between surges in fluorescence.

The peak fluorescence amplitudes of the 90 mmol/l KCl-evoked hotspots, classified as either monophasic or multiphasic exocytosis, were 151 ± 7% ($n = 23$) and 170 ± 9% ($n = 5$), respectively (Fig. 1*A*). The monophasic events contributed to 82% of the exocytic events (Fig. 1*B*), similar to our previous report (8), and the remaining 18% were multiphasic events. Figure 1*C* shows the typical FM1-43 hotspots from a single islet β-cell in response to 90 mmol/l KCl stimulation (see supplemental movie 1, which is detailed in the online appendix [available at http://diabetes.diabetesjournals.org]). Figure 1*D* shows the fluorescence traces of each of the indicated FM1-43 hotspots in Fig. 1*C* (indicated by arrowheads). Hotspots 1 and 2 are monophasic hotspots wherein the FM1-43 fluorescence rises to a transient peak and then drops to basal fluorescence (Fig.

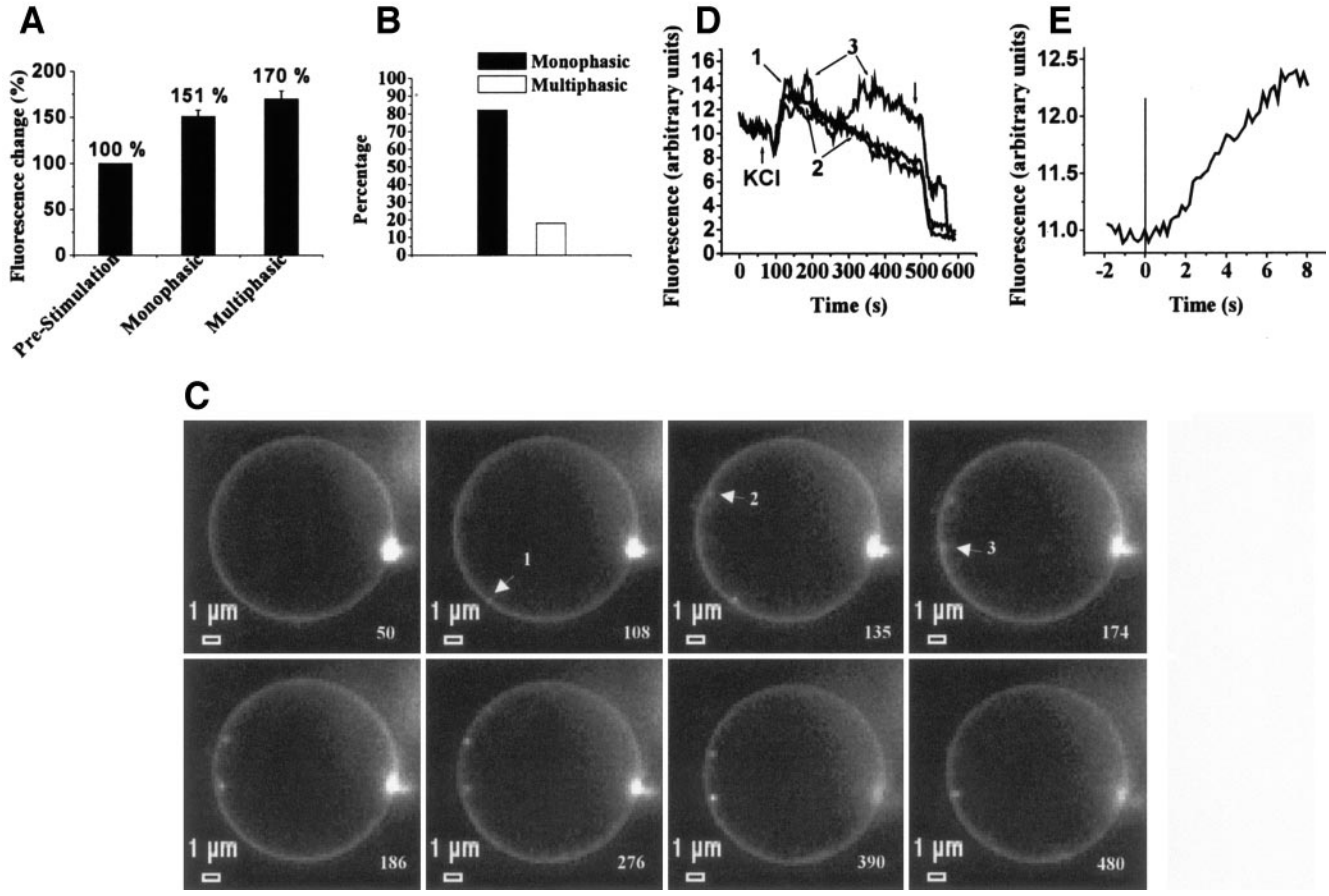

FIG. 1. Exocytosis evoked by KCl depolarization in rat islet β-cells. From Table 1, the exocytotic hotspots from the 16 cells stimulated by 90 mmol/l KCl were analyzed in the following manner. *A*: Average peak fluorescence change of the 28 hotspots (from 16 cells) compared with their prestimulation membrane fluorescence levels. Results are the means ± SE. *B*: Distribution of the hotspots representing monophasic and multiphasic events. *C* and *D*: Representative plasma membrane FM1-43 fluorescence of an islet β-cell is monitored during 90 mmol/l KCl stimulation. *C*: The static images and the times (second) at which the images were captured are indicated on the *bottom right* of each image. Movie 1 shows the real-time imaging at eight frames per second. *D*: The fluorescence traces of the three indicated hotspots (arrows). The time at which KCl was applied is indicated, and the downward arrow indicates when the FM1-43–free nonstimulatory solution was applied to wash out the hotspots, which would indicate that these are exocytic hotspots and not endocytosed vesicles. *E*: Representative example of the fluorescence trace of a multiphasic hotspot from another β-cell monitored at ~5.5 Hz.

1*C* and *D*). In contrast, the fluorescence trace of the multiphasic hotspot 3 displayed a drop from peak fluorescence intensity toward the basal intensity at ~200–250 s, followed by a second surge to a similar peak amplitude followed by a similar drop. These drops in fluorescence intensity likely reflect the active dissolution of the FM1-43 dye to the cell exterior and less likely reflect a transient movement of the hotspot out of the plane of focus because the optical section obtained by the epi-fluorescent microscope is sufficiently thick (8,12). At a much faster image acquisition (~5.5 Hz; Fig. 1*E*), there was a continued and uninterrupted rise to the peak occurring after >10 s, indicating that an earlier peak or decline was not missed in the first 10 s of recording (13), even at the slower image acquisition rate (~0.33 Hz) primarily used in our study. The size of the FM1-43 hotspots was determined by measurement of the pixels at maximal fluorescence intensity. Monophasic hotspots measured to ~507 nm, whereas multiphasic hotspots measured to ~594 nm. The multiphasic hotspots exhibited more variable sizes because the sequentially fused secretory granules are not always precisely in the same plane and could be on top of each other, but were nonetheless captured by the thick optical section. In the latter, the pixel sizes of the fluorescent hotpots would underestimate the actual size of the multigranule fusions. The primary exocytosing secretory granule could be undergoing partial or complete collapse into the plasma membrane as the next secretory granule is fusing with it. The retention of FM1-43 dye within some of these hotspots suggests either that these exocytosing secretory granules did not undergo complete collapse and perhaps reforms ("kiss and run" exocytosis) (12,14,15) or that the dye is sticking to the core matrix, which sometimes sits on the exterior cell surface and does not immediately dissolve (4). In any case, this FM1-43 retention at exocytic sites and increases in fluorescence serve as an excellent indicator for sequential fusion of oncoming secretory granules at the same exocytic sites.

In the absence of IBMX, the membrane FM1-43 exocytic events observed with KCl (as in Fig. 1), or even with the addition of GLP-1 (data not shown), were not always reliable. We therefore added IBMX (150 μmol/l) to the solutions in all succeeding studies. KCl + IBMX resulted in a major redistribution of the exocytic events compared with KCl alone, where multiphasic events increased to 65% and monophasic events were reduced to 35% (Fig. 2*A*). The maximal fluorescence amplitudes of the multiphasic hotspots evoked by KCl + IBMX (251 ± 23%; $n = 17$; Fig.

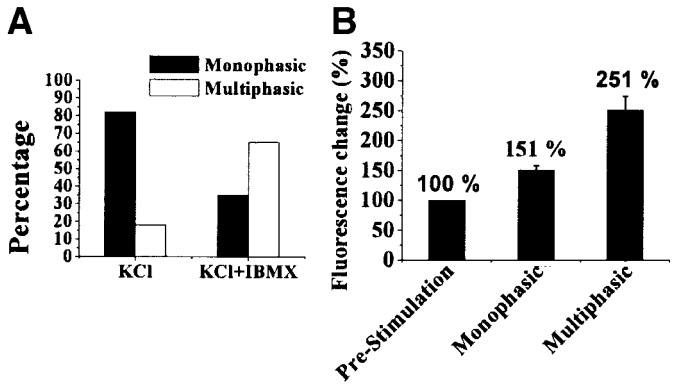

FIG. 2. Exocytosis evoked by KCl + IBMX in rat islet β-cells. From Table 1, the exocytotic hotspots from the 13 islet β-cells evoked by 90 mmol/l KCl + 150 μmol/l IBMX were analyzed in the following manner. *A*: Distribution of the hotspots representing monophasic and multiphasic events: a comparison of KCl + IBMX versus KCl alone (from Fig. 1); *B*: average peak fluorescence change of the 26 hotspots (from 13 cells) compared with their prestimulation membrane fluorescence levels. Results are the means ± SE.

2*B*) were also higher than those evoked by KCl alone (170 ± 9%; $n = 5$; Fig. 2*A*), suggesting that an increase in cytosolic cAMP concentrations by IBMX stimulation potentiated sequential exocytosis. The maximal amplitudes of the monophasic hotspots evoked by KCl + IBMX (151 ± 7%; $n = 9$) or by KCl alone (151 ± 7%; $n = 23$) were remarkably identical. However, KCl + IBMX only minimally increased the number of exocytic events (2.0 ± 0.3 hotspots/cell) at the cell equator ($n = 26$ hotspots from 13 cells) compared with KCl alone (1.8 ± 0.5 hotspots/cell) (Table 1). Therefore, at moderate cAMP stimulation by IBMX alone, there is a preference to increase sequential secretory granule fusions over increasing the number of exocytic sites at the plasma membrane.

GLP-1 stimulation evokes compound exocytosis in rat pancreatic islet β-cells. We then examined exocytosis evoked by maximal cAMP stimulation by GLP-1 (10 nmol/l) on 90 mmol/l KCl + 150 μmol/l IBMX. Remarkably, the number of plasma membrane hotspots increased to 6.0 ± 0.7 ($n = 90$ hotspots from 15 consecutive cells with all cells responding; Table 1), which is approximately three times that of KCl + IBMX or KCl alone. GLP-1 (with KCl + IBMX) caused a major redistribution of the exocytic events (Fig. 3*A* and *B*). Monophasic events constituted only 10% (9 of 90 hotspots from 15 cells), whereas multiphasic events constituted 41% ($n = 37$ of 90 hotspots); and most striking is a novel third pattern of a rapid and robust rise in the membrane FM1-43 fluorescence to a very high amplitude that remained sustained, which constituted the largest portion of 49% (44 of 90 hotspots) of the hotspots. We will call this the "robust and sustained" hotpots. We will now discuss each of these exocytotic patterns.

The robust and sustained hotspots typically exhibit a rapid and robust rise in the membrane FM1-43 fluorescence to a very high amplitude (354 ± 18%; $n = 44$ of 90 hotspots from 15 cells) (Fig. 3*B*). This pattern of exocytosis was distinctly absent in the KCl + IBMX or KCl alone (Fig. 3*A*). Because the peak amplitudes (minus basal fluorescence) of these hotspots (354% − 100% = 254%) is four to five times that of the monophasic hotspots evoked by KCl (151% − 100% = 51%; Fig. 1*A*) or KCl + IBMX (151% − 100% = 51%; Fig. 2*B*), we have initially considered these exocytic events as possible fusions of multiple granules, possibly from already perfused granules, toward a single fusion pore opening, as classically described for compound exocytosis. This of course could not be distinguished from a greatly accelerated sequential granule-granule fusion with this imaging assay.

Figure 3*C* shows the typical FM1-43 hotspots responses from a representative β-cell stimulated with 10 nmol/l GLP-1 (with KCl + IBMX) (see supplemental movie 2 in the online appendix). The bright spot on the upper left on the cell is adherent debris that traps FM1-43, as was similarly observed in chromaffin cells (4), and was excluded from analysis. Overall, the fluorescent hotspots distributed randomly along the equatorial plane of focus, suggesting that the exocytic sites did not seem to preferentially cluster together on the plasma membrane. The majority of these hotspots appeared to "grow" in size. For example, the size of the exocytic hotspot 2 (in Fig. 3*C* and *D*) of the GLP-1 (+ IBMX)–treated β-cell was initially at ~515 nm in diameter (at 174 s in Fig. 3*C*, estimated by the calculated pixel size; see RESEARCH DESIGN AND METHODS), and with KCl stimulation, rapidly grew to a maximum of ~618 nm (at 288 s in Fig. 3*C*). This size-increase pattern was also observed with the multiphasic hotspots (i.e., hotspot 1 in Fig. 3*C* and *D*). The apparent growth in the size of the exocytosing secretory granules seemed considerably less than the increase in fluorescence intensity, in part because the secretory granules could be merging and for other reasons already mentioned above for sequential exocytosis. The fluorescence intensity of most of these hotspots remained relatively sustained during the duration of stimulation (Fig. 3*D*), although some gradually waned by ~30% of the peak fluorescence amplitudes (as with hotspot 2), the latter likely due to dissolution of the FM1-43 into the cell exterior.

The monophasic hotspots evoked by GLP-1 were different from those evoked by KCl (in Fig. 1*A*) or KCl + IBMX (in Fig. 2*B*). The peak amplitudes of GLP-1–evoked monophasic hotspots were much higher at 278 ± 23% (Fig. 3*B*) and actually remarkably similar to the amplitudes of the multiphasic hotspots evoked by KCl + IBMX (Fig. 2*B*) or by GLP-1 (with KCl + IBMX, in Fig. 3*B*). We believe that these GLP-1–evoked monophasic hotspots likely represent either an acceleration of sequential granule fusions or compound exocytosis and are therefore distinct from the smaller monophasic hotspots of single granule fusions evoked by KCl alone. Of note, some of the monophasic events did not appear immediately (<1 min) after stimulation but emerged as late as ~3 min after stimulation. This suggests that these granules were likely being mobilized to the plasma membrane rather than arising from a previously docked pool of secretory granules. GLP-1 stimulation therefore not only promoted secretory granule–secretory granule fusions resulting in sequential and compound exocytoses at exocytic sites that would have otherwise undergone monophasic single granule exocytosis, but also evoked new secretory granule–plasma membrane fusions, indicating a recruitment of new primary exocytic sites.

GLP-1 evoked two multiphasic stepwise patterns of plasma membrane FM1-43 hotspots, indicating sequential

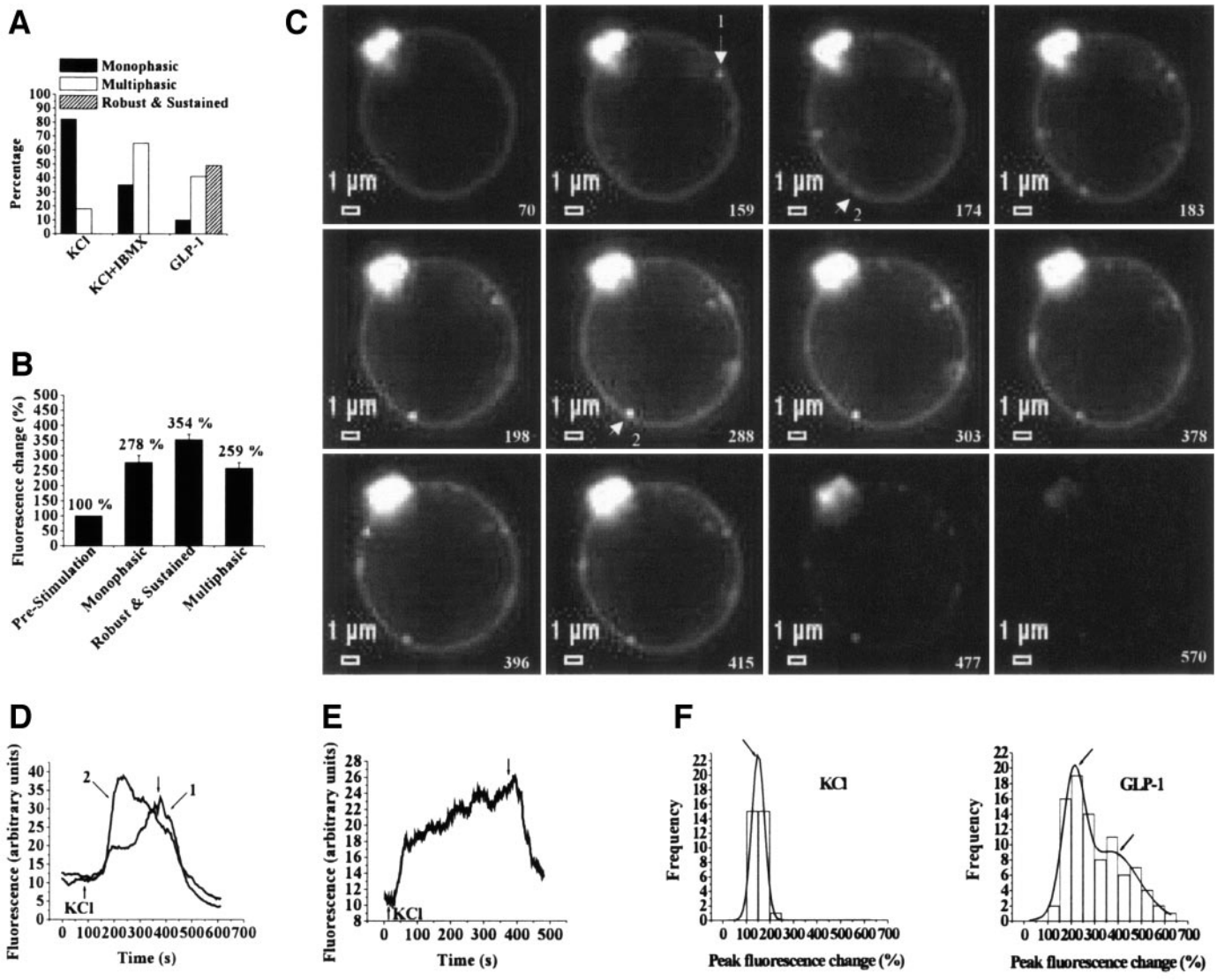

FIG. 3. GLP-1 potentiation of KCl + IBMX–evoked exocytosis in rat islet β-cells. From Table 1, the exocytotic hotspots from the 15 islet β-cells evoked by 90 mmol/l KCl + 150 μmol/l IBMX in the presence of 10 nmol/l GLP-1 were analyzed in the following manner. *A*: Distribution of the hotspots representing monophasic, robust and sustained, and multiphasic events evoked by GLP-1 potentiation (90 hotspots from 15 cells) compared with KCl and KCl + IBMX (from Figs. 1 and 2). Note that GLP-1 potentiation evoked a robust and sustained pattern not observed with KCl or KCl + IBMX stimulation. *B*: Average peak fluorescence change of the GLP-1 potentiated FM1-43 hotspots (90 hotspots/15 cells) compared with their prestimulation membrane fluorescence levels. Results are the means ± SE. *C*: Static images of the FM1-43 fluorescence of a representative islet β-cell stimulated by this protocol. The times (in seconds) at which the images were captured are indicated on the *bottom right* of each image. Arrows indicate the two hotspots that were analyzed in *D*. Supplemental movie 2 shows the real-time imaging of this cell at eight frames per second. *D*: Fluorescence traces of the two indicated hotspots shown in *C*. Downward arrow indicates the time at which FM1-43–free nonstimulatory bath solution was applied. Hotspot 1 is a multiphasic exocytic event showing an orderly stepwise increase in fluorescence. Hotspot 2 is a robust/sustained exocytic event showing a rapid rise to a very high peak followed by a slow decline. *E*: Fluorescent traces of a multiphasic hotspot from another GLP-1–stimulated islet β-cell. Note that the fluorescence plateaus are not as obvious as hotspot 1 in *D* but appear choppy, and the peak amplitude reached is lower. *F*: Profile distribution of maximal fluorescence intensity change (%) of individual hotspots. The smooth lines are drawn according to Gaussian distribution, which showed one peak for KCl and two peaks for GLP-1 (indicated by arrows). The *left panel* analyzed the 31 hotspots from 17 cells stimulated with 90 mmol/l KCl. The *right panel* analyzed the 90 hotspots from 15 cells stimulated by 10 nmol/l GLP-1 (with 90 mmol/l KCl + 150 μmol/l IBMX).

exocytosis (8). The first pattern (11 of 37 hotspots) was that of plateaus separating fluorescence rises (Fig. 3*D*, hotspot 1), similar to that of multiphasic hotspots evoked by KCl alone (Fig. 1*D*, hotspot 3). The peak fluorescence levels reached were 323 ± 32%, similar to the peak amplitudes reached by the robust/sustained hotspots (Fig. 3*B* and *D*, hotspot 2). This would suggest that the number of secretory granules fused at these sequential exocytic sites was similar to those occurring during compound exocytosis. In the second more prevalent pattern (26 of 37 hotspots), the plasma membrane FM1-43 fluorescence initial increase was rapid, but the subsequent rises to the peak was erratic or "choppy," without clear plateaus between the peaks (Fig. 3*E*). Here, the peak amplitudes were lower, reaching only 230 ± 29%. When the data of both types of sequential exocytoses were combined, the peak amplitudes were 259 ± 18% (Fig. 3*B*). These different patterns likely reflect different kinetics of sequential secretory granule–secretory granule fusions evoked by GLP-1, KCl, and also glucose (8). Alternatively, the choppy appearance of the plateaus could be due to different patterns of granule content emptying patterns evoked by the dif-

ferent agonists, although the FM1-43 assay is not an accurate indicator of granule content emptying.

To further assess the occurrence of compound and sequential exocytosis (16), we plotted the distribution of the maximal fluorescence intensity change (percentage) of individual hotspots (Fig. 3*F*). According to Gaussian distribution, the fluorescence intensity of the hotspots evoked by KCl is well fit with only one peak (indicated by arrow) with a low fluorescence intensity change of 149%, which suggests that the majority of monophasic events are of single secretory granule exocytosis. With GLP-1 stimulation, the Gaussian distribution shows two peaks (indicated by arrows) corresponding to much higher fluorescence intensity changes of 211 and 372%. These two peaks appear quantal, which would represent the fusions of at least two (or three) insulin secretory granules. The sequential patterns of fluorescence intensity rises to these peaks indicate a gradual incorporation of secretory granule membranes, which would suggest sequential secretory granule–secretory granule fusions, whereas a robust rapid rise to a high fluorescence intensity peak would suggest multigranule fusions or compound exocytosis (or acceleration of sequential exocytosis).

Ultrastructural evidence of granule-granule fusions in the islet β-cell. The FM1-43 dye records only the behavior of an exocytosing secretory granule but not the insulin secretory granule dynamics before exocytosis with the plasma membrane. Previous studies using patch-clamp capacitance measurements to examine the potentiating actions of cAMP, including GLP-1 stimulation, on secretory granule pool mobilization and priming (17,18) also lacked the ultrastructural information to support the conclusions. We therefore perform electron microscopy to provide "snapshots" of the precise insulin secretory granule behavior inside the cell and those undergoing exocytosis, and such insights would complement and/or confirm those insights derived from the real-time FM1-43 imaging assay. Here, rat islet β-cells were stimulated with KCl + IBMX in the absence or presence of GLP-1 for 3 min and then fixed for electron microscopy study.

Because priming of insulin secretory granules for ready release takes place after the insulin secretory granules are physically docked onto the plasma membrane (17,19), we predicted that GLP-1 potentiation of KCl + IBMX stimulation would result in an increase in the number of physically docked insulin secretory granules. Here, insulin secretory granules were considered as physically docked if they were in direct contact with the plasma membrane (Fig. 4*A*). In the presence of GLP-1, the number of physically docked secretory granules in the islet β-cells was ~2.2 times more than KCl + IBMX alone (7.5 ± 0.9 secretory granules/μm^2; $n = 23$ cell sections vs. 3.4 ± 0.3 secretory granules/μm^2; $n = 12$ cell sections, $P < 0.05$; Fig. 4*B*). We recognize that some of the physically docked secretory granules would appear not to be in direct contact with the plasma membrane because of random sectioning (10). To confirm that this did not preferentially underestimate the number of physically docked secretory granules, we have used an electron microscopy analysis described by Olofsson et al. (11), in which the number of physically docked secretory granules was estimated as 13% of all the insulin secretory granules situated within 120 nm (i.e., one-half of the mean profile granule diameter [see below and Fig. 4*C*]) of the plasma membrane (11). Using this analysis to negate any bias, GLP-1 potentiation resulted in 16.8 ± 1.6 secretory granules/μm^2 ($n = 23$ cells; Fig. 4*B*), whereas KCl + IBMX alone resulted in 10.4 ± 1.1 secretory granules/μm^2 ($n = 12$ cells, $P < 0.05$; Fig. 4*B*). Here, the extra number of physically docked secretory granules accounted for was smaller for KCl + IBMX alone (10.4 secretory granules/μm^2 × 13% = 1.35 secretory granules/μm^2) compared with the presence of GLP-1 (16.8 secretory granules/μm^2 × 13% = 2.18 secretory granules/μm^2) (Fig. 4*B*). This analysis would also assume that 87% of the accounted secretory granules would not be physically docked but would nonetheless be very close to the plasma membrane, which would suggest an increase in secretory granule mobilization toward the plasma membrane. This increased secretory granule mobilization to within 120 nm of the plasma membrane caused by GLP-1 potentiation was ~1.6 times (i.e., 16.8/10.4 = 1.61) that caused by KCl + IBMX alone. These results were not due to miscounting/overcounting of insulin secretory granules that may happen with random sectioning, because the mean secretory granule diameters calculated from all the insulin secretory granules counted using a method described by Giger and Riedwyl (10) were similar (KCl + IBMX alone, 320 ± 6 nm; $n = 1988$ secretory granules from 12 cell sections vs. GLP-1 potentiation, 310 ± 6 nm; $n =$ 3,385 secretory granules from 14 cell sections; Fig. 4*C*). Altogether, these results suggested that GLP-1 potentiation not only increased the number of insulin secretory granules to physically dock onto the plasma membrane but also increased the mobilization of more secretory granules to approach the plasma membrane, presumably to eventually participate in exocytosis.

Next, we hypothesized that GLP-1 stimulation would enhance secretory granule–to–secretory granule fusions at the plasma membrane. Secretory granule–secretory granule fusions were increased by cAMP stimulation in rat pituitary lactotrophs (20). We determined the number of events in which an insulin secretory granule is in direct contact with a secretory granule that is physically docked (docked granule-granule [DGG] fusion; Fig. 4*D*) or appearing as being exocytosed (exocytosing granule-granule [EGG] fusion; Fig. 4*E*, *1*–*3*). An insulin secretory granule was considered as being exocytosed if *1*) the secretory granule membrane is continuous with the plasma membrane (Fig. 4*E*, *1*, *2*, *4*, and *5*) with a patent secretory granule pore communicating with the cell exterior, *2*) the physically docked secretory granule is distorted with partial emptying of its dense core contents (Fig. 4*E*, *2* and *3*), or *3*) the secretory granule is protruding onto the plasma membrane as if to be forming a fusion pore with the plasma membrane (Fig. 4*E*, *6*). To avoid an overlap in the counting of these two secretory granule–secretory granule fusion events, if both exocytosing granule(s) and docked granule(s) were involved in a single multigranule fusion event, this would be counted only once as an EGG(s) fusion event. When the DGG and EGG fusion events were tallied together (DGG + EGG; Fig. 4*F*, top), we found that GLP-1 potentiation greatly increased such secretory granule–secretory granule fusion events at the plasma membrane by ~2.8-fold compared with KCl +

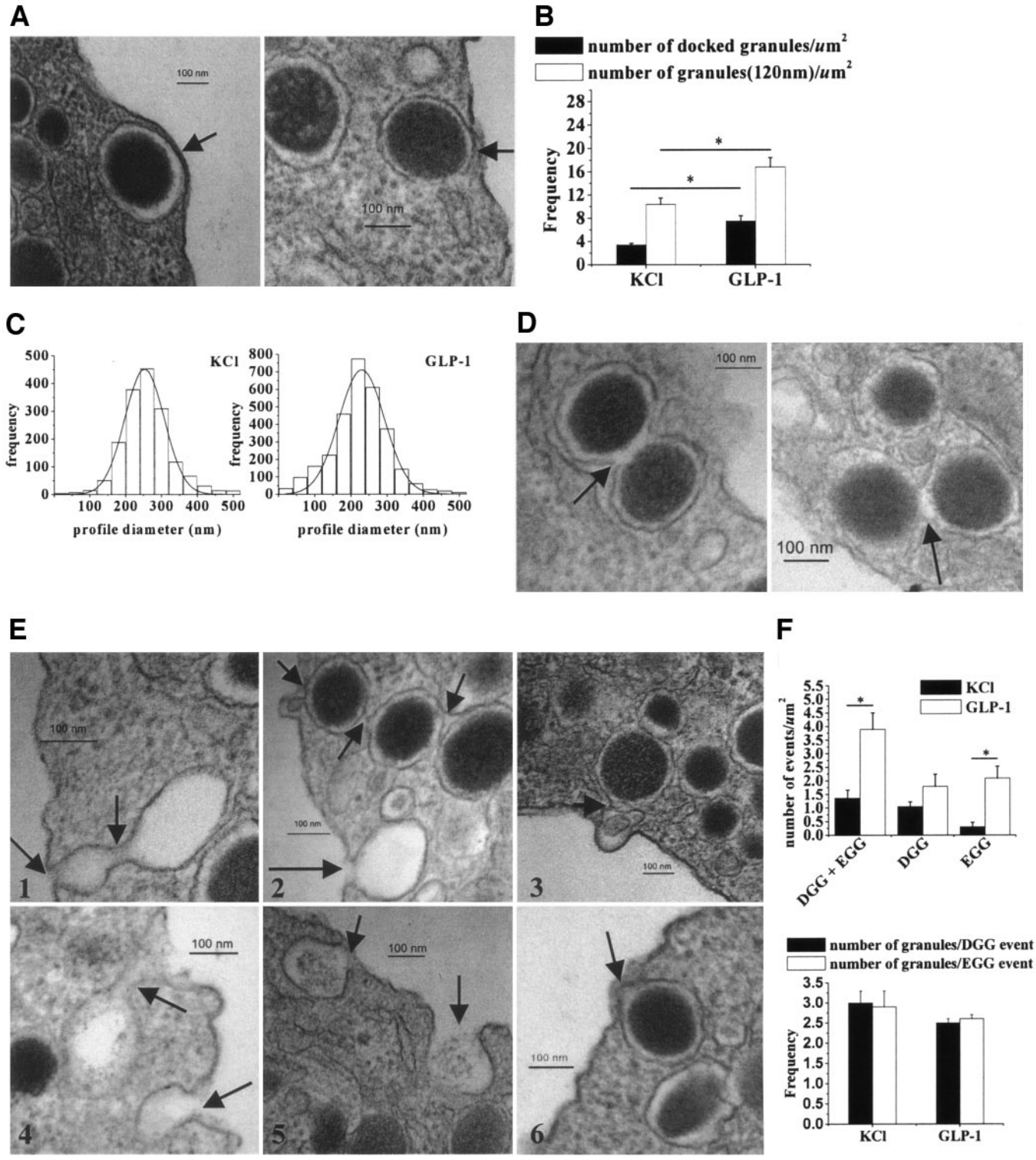

FIG. 4. Ultrastructural analysis of KCl + IBMX–evoked exocytosis in islet β-cells in the absence and presence of GLP-1 potentiation. *A*: These β-cells were stimulated with GLP-1 (with KCl + IBMX). The insulin secretory granules indicated by arrows are physically docked onto, but do not distort, the plasma membrane. *B*: Histogram of the number of docked secretory granules evoked by KCl + IBMX in the absence or presence of GLP-1. Solid bars show the number of secretory granules actually docked on the plasma membrane, and open bars show the number of secretory granules located within 120 nm of the plasma membrane, excluding those secretory granules counted as docked (solid bars). *C*: Profile of measured insulin secretory granule diameter. The diameters of the insulin secretory granules were determined (GLP-1 [with KCl + IBMX], n = 1,988 secretory granules from 12 micrographs; KCl [with IBMX], n = 3,385 secretory granules from 14 micrographs), and the frequency of their occurrence was analyzed. The smooth line is drawn according to Gaussian distribution showing a similar pattern between GLP-1 (KCl+ IBMX) and KCl (+ IBMX) stimulation and with similar mean secretory granule diameters of 310 ± 6 nm and 320 ± 6 nm, respectively. *D*: Both *left* and *right panels* show two secretory granules in contact with each other (indicated by arrows) that are involved in a DGG fusion event. Note that the docked granule does not distort the plasma membrane. *E*: Exocytosing granules. *1*, *2* (lowest arrow), *4*, and *5*: Secretory granule membrane continuous with the plasma membrane with emptying of contents. *2* (top left arrow) and *3*: Secretory granule distorting the plasma membrane (also partially emptied). *6*: Granule protruding onto the plasma membrane. *1*, *2* (top center and right arrows), and *3*: Also note that the granular membranes of secretory granules fuse together in the EGG fusion events. The smaller exocytosing secretory granules in *2* and *3* have partially

IBMX alone (3.9 ± 0.6 events/μm^2; n = 23 cell section vs. 1.4 ± 0.3 events/μm^2; n = 12 cell section, $P < 0.05$). When the granule-granule fusion events were analyzed independently (Fig. 4*F*, *top*), we find that a larger proportion (54%) of these secretory granule–secretory granule fusions in the GLP-1 potentiation were actually undergoing exocytosis (EGG, 2.1 ± 0.4 events/μm^2; n = 23 cell sections) compared with those that were only physically docked (DGG, 1.8 ± 0.4 events/μm^2; n = 23 cell sections), which is 46%. In contrast, for the KCl + IBMX stimulation alone, only a small proportion (21%) of the secretory granule–secretory granule fusion events were undergoing exocytosis at the plasma membrane (EGG, 0.3 ± 0.2 events/μm^2, n = 12 cell sections), whereas the great majority (79%) remained docked (DGG, 1.1 ± 0.2 events/μm^2, n = 12 cell sections). GLP-1 potentiation caused a remarkable approximately seven times more EGG fusion events than KCl + IBMX alone (EGG in Fig. 4*F*, *top*, 2.1/0.3, $P < 0.05$). This would explain the larger number (threefold increase) in FM1-43 exocytic hotspots caused by GLP-1 potentiation over that of KCl + IBMX alone (Table 1). Surprisingly, the number of secretory granules involved in the EGG or DGG fusion events (Fig. 4*F*, bottom), either in the absence or presence of GLP-1 potentiation, was similar. The latter would explain two observations in the FM1-43 study for GLP-1 potentiation. First is the similar peak amplitudes of the GLP-1–potentiated responses (multiphasic and monophasic hotspots; Fig. 3*C*) compared with the multiphasic FM1-43 responses of KCl + IBMX (Fig. 2*B*). Second, GLP-1 must have greatly accelerated secretory granule–secretory granule fusion events with the exocytosing secretory granules over those caused by KCl + IBMX alone, and this very rapid secretory granule–secretory granule fusion might explain the even higher amplitudes attained by the robust/sustained FM1-43 hotspots (Fig. 3*C*). The remaining number of DGG fusion events (DGG; Fig. 4*F*, *top*) caused by GLP-1 potentiation showed only a tendency toward being more than KCl + IBMX alone (1.8 ± 0.4 secretory granules/μm^2, n = 23 cell sections; vs. 1.1 ± 0.2 secretory granules/μm^2, n = 12 cell sections, P = 0.24). We also determined the number of homotypic fusion events in which two or more granules (at least one of them was situated within 120 nm of the plasma membrane) are fusing together but none of them are docked or exocytosing. Here, GLP-1 potentiation induced a tendency toward having more of these events (supplemental Fig. 1*S*, *left*, in the online appendix; 3.1 ± 0.6 events/μm^2, n = 23 cell sections; vs. 1.8 ± 0.4 events/μm^2, n = 12 cell sections, P = 0.15). It therefore appears that GLP-1 acted more to promote the docked secretory granules to fuse with the plasma membrane (EGG in Fig. 4*F*, *top*) more so than inducing homotypic secretory granule–secretory granule fusion (Fig. 4*F*, *bottom*; supplemental Fig. 1*S*, *left*, in the online appendix). Initial secretory granule–plasma membrane fusion (primary exocytosis) does not seem to be required for subsequent secretory granule–secretory granule fusions to occur (Fig. 4*D*), and in fact, a very substantial 46% of the secretory granule–secretory granule fusion events evoked by GLP-1 potentiation were of the physically docked type (DGG in Fig. 4*F*, *top*) and not undergoing exocytosis (i.e., EGG). The latter would suggest that compound exocytosis would also occur and is promoted by the GLP-1 potentiation.

DISCUSSION

In this study, we show the different exocytic events that account for GLP-1 potentiation of Ca^{2+}-mediated insulin secretion. First, we show an increase in the mobilization of granules to approach and dock at the plasma membrane. Specifically, the electron microscopy study shows that GLP-1 potentiation caused a 1.6 times increase in the number of insulin secretory granules within 120 nm of the plasma membrane when compared with KCl + IBMX alone. The number of insulin secretory granules actually docked on the plasma membrane was increased by 2.2 times. Using electron microscopy, Straub et al. (21) recently showed that glucose stimulation increased the number of docked insulin secretory granules by twofold in a manner independent of $[Ca^{2+}]_i$. Hence, our data suggest that GLP-1 stimulation would potentiate an even greater increase in the number of docked secretory granules and therefore increases the likelihood of these docked secretory granules to be released. Presumably, GLP-1 also upregulated the priming steps to render these docked secretory granules to become readily releasable (22). Second, GLP-1 potentiation caused an increase in the number of exocytic sites at the plasma membrane. The FM1-43 study shows that GLP-1 potentiation caused a threefold increase in exocytic sites compared with KCl + IBMX and a sixfold increase when compared with KCl alone. When these exocytotic sites were examined in greater detail by electron microscopy for the number of multigranule fusion events actually undergoing exocytosis, GLP-1 caused a remarkable seven times increase over that of KCl + IBMX alone. Third and importantly, GLP-1 potentiation caused an acceleration of sequential and compound exocytosis on the basis of the behavior of the multigranule fusion events. We admit that we cannot completely distinguish whether the multigranule fusion events we observed represent sequential versus compound exocytosis. To reiterate, sequential exocytosis is defined by the initial exocytosis of a secretory granule with the plasma membrane followed by an orderly and single fusion of oncoming secretory granules with the exocytosing secretory granules (23). Compound exocytosis is defined as the fusion of multiple secretory granules, frequently perfused in the cytosol (homotypic fusion), into a single exocytotic fusion pore opening on the plasma membrane (24). On electron microscopy, compound exocytosis is characteristically observed as multiple secretory granule cores enclosed in a single membrane in the process of exiting through a single membrane pore, which is actually rarely observed here or in previous reports (25).

emptied their contents and protrude onto the plasma membrane. *F*: *Top panel* shows the analysis of docked (DGG as in *D*) and exocytosing (EGG as in *E*, *1*, *2* [*top center* and right arrows], and *3*) secretory granule–secretory granule fusion events. The histogram shows the DGG and EGG events analyzed together and separately, and shown as events per square micrometer. Note that the GLP-1 evoked many more EGG events. *Bottom panel* shows the number of insulin secretory granules involved in each DGG and EGG event, which is similar between GLP-1 and KCl. These studies were obtained from dispersed single cells of islets (~200 islets/rat) isolated independently from each of four rats.

On FM1-43 imaging capable of visualizing exocytosis in real-time, sequential exocytosis is best observed as a stepwise (multiphasic) increase in the membrane hotspot to a stable peak amplitude, and is the dominant response in KCl + IBMX, as well as with glucose stimulation that we previously reported (8). Takahashi et al. (16) recently provided evidence of sequential exocytosis of insulin secretory granules using two-photon excitation imaging. However, with GLP-1 potentiation, we also observed larger amplitude rises in both monophasic and robust/sustained hotspots, which were of similar (monophasic) or higher amplitudes (robust/sustained) attained by the multiphasic responses evoked by KCl + IBMX alone. We interpret these FM1-43 imaging results against the electron microscopy results to indicate that the process of sequential secretory granule–secretory granule fusions must be greatly accelerated by GLP-1. Presumably, the milder cAMP stimulation of the KCl + IBMX promoted a slower rate of sequential exocytosis. The appearance of a "chain of fusion granules" (DGG in Fig. 4*D* and EGG in Fig. 4*E*, *top*), which is the dominant observation in KCl + IBMX stimulation and with GLP-1 potentiation, supports the process of sequential exocytosis. This interpretation of our FM1-43 results, which is consistent with the report by Takahashi et al. (16), also supports this thinking of sequential exocytosis.

We do recognize, however, that the FM1-43 assay tracks only the insulin secretory granules that are actually undergoing exocytosis (8). If FM1-43 were to stain vesicular membranes by means of diffusion through the cytosol of the vesicles, this would result in wider fusion sacs to more convincingly show classic compound exocytosis, which could be further distinguished from accelerated sequential exocytosis by an even more abrupt and higher increase in FM1-43 fluorescence. However, FM1-43 was reported to more likely stain the lipid membrane by unrestricted lateral diffusion through the membrane than by aqueous diffusion (13), and therefore, the kinetics of the rising phase of FM1-43 fluorescence might be similar between these exocytic processes. Although our FM1-43 results could be interpreted to suggest that the GLP-1–mediated large amplitude rises are less likely to be due to perfused granules (as in the case with compound exocytosis) but an acceleration of sequential exocytosis, we certainly cannot rule out a major occurrence of compound exocytosis. In fact, our electron microscopy study showed that a substantial 46% of the secretory granule–secretory granule fusion events at the plasma membrane are docked but not yet undergoing exocytosis, indicating that prefusion of secretory granules before exocytosis must also be occurring. Some of the large amplitude robust/sustained hotspots could therefore be true compound exocytosis. Assuming that insulin secretory granule mobilization occurs at comparable speed in sequential and compound exocytosis and that the lateral diffusion of FM1-43 within the plasma membrane is unrestricted, the robust increase in FM1-43 fluorescence characterizing compound exocytosis may likely be explained by secretory granule–secretory granule (homotypic) fusions having already taken place inside the cell before their fusions to the plasma membrane. This type of exocytosis is predominant in peritoneal mast cells (26). We in fact observed secretory granule–secretory granule fusions deep in the β-cell cytoplasm (supplemental Fig. 1*S*, *middle* and *right*, in the online appendix) as well as close to the plasma membrane, but these events were not much more frequent with GLP-1 potentiation (supplemental Fig. 1*S*, *left*, in the online appendix). The pattern of robust/sustained FM1-43 hotspots constituted a dominating ~50% of the hotspots caused by GLP-1 potentiation (Fig. 3*A*).

The exocytosing secretory granules do not appear to always completely collapse with the plasma membrane but rather form small fusion pores (Fig. 4*E*, *1* and *2*), supporting the possibility that some of these fusion pore openings might be transient and would retract and close, supporting the kiss and run type of insulin exocytosis postulated by Tsuboi et al. (14,15). Here, cargo emptying may not be complete (Fig. 4*E*, *3*), suggesting a mechanism of metered emptying of cargo. Also, if these secretory granules do not undergo complete collapse with the plasma membrane, they could serve as depots for further replenishment of granule content cargo without the need for de novo generation of entirely new secretory granules. As well, this would conserve and reuse the low abundance granule membrane exocytic fusion machinery proteins (SNARE proteins) of the β-cell. Lastly, it would not be necessary for secretory granule situated deep inside the cell to traverse all the way to the plasma membrane but rather to be targeted to the primary exocytosing secretory granules, which serve as docking/fusing sites for these secondary sequentially fusing secretory granules. This in turn would suggest that the exocytic machinery mediating the secondary secretory granule–secretory granule fusions are likely to be distinct from that mediating primary exocytosis. Takahashi et al. (16) showed by two-photon excitation imaging that SNARE protein SNAP-25 (tagged to GFP) on the plasma membrane could redistribute into the insulin secretory granule membrane when the fusion pore opens during sequential secretory granule–secretory granule fusions, but not during primary exocytosis of insulin secretory granule with the plasma membrane. Takahashi's study also showed the sequential exocytosis of insulin secretory granules to be less frequent (<10% of all exocytic events) than our study. This discrepancy could in part be explained by the fact that their study was conducted on β-cells within intact mouse islets, which may be subject to paracrine inhibition (somatostatin) and autocrine inhibition (insulin) (27), whereas our experiments were performed on single rat β-cells. Also, mouse islets are less vigorous secretors with a very low sustained phase of insulin secretion compared with rat islets (used in our study).

Our study therefore indicates that the increased cAMP activation by GLP-1 stimulation enhanced secretory granule–secretory granule and secretory granule–plasma membrane fusions to account for the acceleration of sequential and/or compound exocytosis. In rat pituitary lactotrophs, cAMP activation increased secretory granule–secretory granule fusion but not the number of plasma membrane fusion events evoked by KCl stimulation, whereas the latter was selectively enhanced by protein kinase C activation (20). In horse eosinophils, protein kinase C did not exhibit any such effects (28), but instead, GTPγS, a nonhydrolyzable GTP analog, induced secretory granule–

secretory granule fusions and compound exocytic events while reducing the number of exocytic sites (29,30). GTPγS stimulation was shown to potentiate insulin exocytosis in a cAMP- and Ca^{2+}-dependent manner (31), but it remains unknown as to which molecular substrate or exocytic event is modulated by GTPγS. Furthermore, the molecular regulation of these exocytic events in the islet β-cells and other secretory cells (chromaffin cell, lactotrophs, and eosinophils) are also likely to be different. Insulin secretory granule-to-plasma membrane fusion and secretory granule-to-secretory granule fusion may therefore require distinct requirements of GTP, cAMP, and Ca^{2+} and, very likely, distinct molecular substrates for these cellular signals. It would be of interest in the more effective treatment of diabetes to elucidate the precise underlying molecular mechanisms by which GLP-1 potentiation, perhaps in part via these cellular signals, is coupled to sequential and compound insulin exocytosis.

ACKNOWLEDGMENTS

H.G. has received Canadian Institute for Health Research Grant (CIHR) MOP-64465, Canadian Diabetes Association Grant 1630, and an equipment grant from the Banting and Best Diabetes Center of the University of Toronto. E.K. has received a Banting and Best Diabetes Centre/Novo Nordisk Studentship and a CIHR Canada Graduate Scholarships Doctoral Award.

We thank X. Gao and Steve Doyle for technical assistance and R. Tsushima for active discussion.

REFERENCES

1. Drucker DJ: Glucagon-like peptides. *Diabetes* 47:159–169, 1998
2. MacDonald PE, El-Kholy W, Riedel MJ, Salapatek AM, Light PE, Wheeler MB: The multiple actions of GLP-1 on the process of glucose-stimulated insulin secretion. *Diabetes* 51 (Suppl. 3):S434–S442, 2002
3. Ding WG, Gromada J: Protein kinase A-dependent stimulation of exocytosis in mouse pancreatic β-cells by glucose-dependent insulinotropic polypeptide. *Diabetes* 46:615–621, 1997
4. Smith CB, Betz WJ: Simultaneous independent measurement of endocytosis and exocytosis. *Nature* 380:531–534, 1996
5. Betz WJ, Bewick GS: Optical analysis of synaptic vesicle recycling at the frog neuromuscular junction. *Science* 255:200–203, 1992
6. Ryan TA, Smith SJ: Vesicle pool mobilization during action potential firing at hippocampal synapses. *Neuron* 14:983–989, 1995
7. Angleson JK, Cochilla AJ, Kilic G, Nussinovitch I, Betz WJ: Regulation of dense core release from neuroendocrine cells revealed by imaging single exocytic events. *Nat Neurosci* 2:440–446, 1999
8. Leung YM, Sheu L, Kwan E, Wang G, Tsushima R, Gaisano H: Visualization of sequential exocytosis in rat pancreatic islet beta cells. *Biochem Biophys Res Commun* 292:980–986, 2002
9. Leung YM, Kang Y, Gao X, Xia F, Xie H, Sheu L, Tsuk S, Lotan I, Tsushima RG, Gaisano HY: Syntaxin 1A binds to the cytoplasmic C terminus of Kv2.1 to regulate channel gating and trafficking. *J Biol Chem* 278:17532–17538, 2003
10. Giger H, Riedwyl H: Bestimmung der Grössenverteilung von Kugeln aus Schnittkreisradien. *Biometr Zeitschr* 12:156–160, 1970
11. Olofsson CS, Gopel SO, Barg S, Galvanovskis J, Ma X, Salehi A, Rorsman P, Eliasson L: Fast insulin secretion reflects exocytosis of docked granules in mouse pancreatic B-cells. *Pflugers Arch* 444:43–51, 2002
12. Aravanis AM, Pyle JL, Harata NC, Tsien RW: Imaging single synaptic vesicles undergoing repeated fusion events: kissing, running, and kissing again. *Neuropharmacology* 45:797–813, 2003
13. Takahashi N, Kishimoto T, Nemoto T, Kadowaki T, Kasai H: Fusion pore dynamics and insulin granule exocytosis in the pancreatic islet. *Science* 297:1349–1352, 2002
14. Tsuboi T, Zhao C, Terakawa S, Rutter GA: Simultaneous evanescent wave imaging of insulin vesicle membrane and cargo during a single exocytotic event. *Curr Biol* 10:1307–1310, 2000
15. Tsuboi T, Rutter GA: Multiple forms of "kiss-and-run" exocytosis revealed by evanescent wave microscopy. *Curr Biol* 13:563–567, 2003
16. Takahashi N, Hatakeyama H, Okado H, Miwa A, Kishimoto T, Kojima T, Abe T, Kasai H: Sequential exocytosis of insulin granules is associated with redistribution of SNAP25. *J Cell Biol* 165:255–262, 2004
17. Gillis KD, Misler S: Enhancers of cytosolic cAMP augment depolarization-induced exocytosis from pancreatic B-cells: evidence for effects distal to Ca2+ entry. *Pflugers Arch* 424:195–197, 1993
18. Renstrom E, Eliasson L, Rorsman P: Protein kinase A-dependent and -independent stimulation of exocytosis by cAMP in mouse pancreatic B-cells. *J Physiol* 502:105–118, 1997
19. Barg S, Eliasson L, Renstrom E, Rorsman P: A subset of 50 secretory granules in close contact with L-type Ca2+ channels accounts for first-phase insulin secretion in mouse beta-cells. *Diabetes* 51 (Suppl. 1):S74–S82, 2002
20. Cochilla AJ, Angleson JK, Betz WJ: Differential regulation of granule-to-granule and granule-to-plasma membrane fusion during secretion from rat pituitary lactotrophs. *J Cell Biol* 150:839–848, 2000
21. Straub SG, Shanmugam G, Sharp GW: Stimulation of insulin release by glucose is associated with an increase in the number of docked granules in the β-cells of rat pancreatic islets. *Diabetes* 53:3179–3183, 2004
22. Straub SG, Sharp GW: Glucose-stimulated signaling pathways in biphasic insulin secretion. *Diabetes Metab Res Rev* 18:451–463, 2002
23. Nemoto T, Kimura R, Ito K, Tachikawa A, Miyashita Y, Iino M, Kasai H: Sequential-replenishment mechanism of exocytosis in pancreatic acini. *Nat Cell Biol* 3:253–258, 2001
24. Bokvist K, Holmqvist M, Gromada J, Rorsman P: Compound exocytosis in voltage-clamped mouse pancreatic beta-cells revealed by carbon fibre amperometry. *Pflugers Arch* 439:634–645, 2000
25. Orci L, Malaisse W: Hypothesis: single and chain release of insulin secretory granules is related to anionic transport at exocytotic sites. *Diabetes* 29:943–944, 1980
26. Alvarez DT, Fernandez JM: Compound versus multigranular exocytosis in peritoneal mast cells. *J Gen Physiol* 95:397–409, 1990
27. Gopel S, Zhang Q, Eliasson L, Ma XS, Galvanovskis J, Kanno T, Salehi A, Rorsman P: Capacitance measurements of exocytosis in mouse pancreatic alpha-, beta- and delta-cells within intact islets of Langerhans. *J Physiol* 556:711–726, 2004
28. Scepek S, Coorssen JR, Lindau M: Fusion pore expansion in horse eosinophils is modulated by Ca2+ and protein kinase C via distinct mechanisms. *EMBO J* 17:4340–4345, 1998
29. Hafez I, Stolpe A, Lindau M: Compound exocytosis and cumulative fusion in eosinophils. *J Biol Chem* 2003
30. Scepek S, Lindau M: Focal exocytosis by eosinophils: compound exocytosis and cumulative fusion. *EMBO J* 12:1811–1817, 1993
31. Proks P, Eliasson L, Ammala C, Rorsman P, Ashcroft FM: Ca(2+)- and GTP-dependent exocytosis in mouse pancreatic beta-cells involves both common and distinct steps. *J Physiol* 496:255–264, 1996